Enhancing Performance of Stretchable and Transparent Triboelectric Nanogenerator by Optimizing Hydrogel Ionic Electrode Property

Xin Jing[a], Heng Li[c], Hao-Yang Mi[a,b], Pei-Yong Feng[a], Xiaoming Tao[d], Yuejun Liu[a]*, Chuntai Liu[b], Changyu Shen[b]*

[a] Key Laboratory of Advanced Packaging Materials and Technology of Hunan Province, Hunan University of Technology, Zhuzhou, 412007, China

[b] Key Laboratory of Materials Processing and Mold, Zhengzhou University, Zhengzhou, 450000, China

[c] Department of Building and Real Estate, Hong Kong Polytechnic University, Hong Kong, 518000, China

[d] Institute of Textile and Clothing, Hong Kong Polytechnic University, Hong Kong, 999077, China

Corresponding Authors:

H.Y. Mi E-mail: mihaoyang@zzu.edu.cn

Y. Liu E-mail: yjliu_2005@126.com

Note:

The authors declare no competing financial interest.

Abstract:

Triboelectric nanogenerators (TENGs) with high transparency and stretchability are desired for invisible and adaptable energy harvesting and sensing. Hydrogel-based TENGs (H-TENG) have shown promising attributes towards flexible and transparent devices. However, the effect of hydrogel property on the triboelectric performance of H-TENG is rarely investigated. Herein, dual-network hydrogels composed of dual-crosslinked polyvinyl alcohol (PVA) and sodium alginate (SA) were synthesized and used as ionic electrodes in H-TENGs. The elasticity of the hydrogel was controlled by varying the concentration of SA, and the distinct influence of hydrogel viscoelastic property on H-TENG performance was verified for the first time. The optimum H-TENG was fabricated by tuning the conductivity and viscoelasticity of PVA/SA hydrogel. The optimum H-TENG possesses high transparency (over 90%) and stretchability (over 250%), and peak output voltage and current of 203.4 V and 17.6 μA, respectively. Specially designed polydimethylsiloxane (PDMS) bag effectively prevents hydrogel dehydration and maintain a stable output in continuous operation. The H-TENG achieved a power density of 0.98 W/m^2 on a 4.7 MΩ external resistor. The H-TENG could easily light 240 green and blue LEDs simultaneously, and demonstrated capability to power small electronics, such as a digital timer and pedometer. This study provides insights into the influence of hydrogel property on H-TENG performance and gives guidance for designing and fabrication of highly stretchable and transparent TENGs.

Keywords: Hydrogel; Dual network; Viscoelasticity; Triboelectric nanogenerator; Energy Harvesting

1. Introduction

Seeking new green sustainable energy resources is an eternal mission for the human being. Traditional green energy generation techniques, like hydroelectric generation, wind generation, and photovoltaic generation, involve large equipment, facilities, and space. [1-3] Mechanical energy harvesting from nature and human daily life using small devices is becoming a rising hot field in the past decade. Among all mechanical energy harvesting technologies, triboelectric nanogenerator (TENG) is capable to harness ubiquitously chaotic mechanical energy from almost all mechanical motions ranging from the sound wave from human talking to the tremendous ocean wave. [4-8] Depending on the type, intensity, frequency, and environment of different mechanical motions, various TENGs have been developed to harvest energy from these motions. [9-11] In the meantime, the emergence of next-generation wearable electronics has attracted immense enthusiasm for the development of flexible, transparent, and self-healable electronic devices. [12-14] In particular, flexible transparent devices that can be perfectly integrated on the substance surface without interfering its appearance and property are highly desired.[15] Developing TENG with high transparency and flexibility is an ongoing demand for improving device adaptive ability and human comfortability when been used for human motion energy harvesting.

Recently, great efforts have been made to develop stretchable and transparent TENGs. A straightforward approach is applying a conductive coating on stretchable triboelectric materials as electrodes of the TENG. [16] Silver nanowires (NWs), PEDOT:PSS, and graphene have been heavily used as the conductive coating layer. [17-18] However, the delamination of the relative rigid layer when the TENG is subjected to deformation is a critical problem limiting the long term stability of the device. [19-21] Flexible ionic conductors are alternative stretchable electrodes for stretchable and transparent TENGs. [22] Different from metallic and polymeric conductors, ionic conductors transfer charge by ions within polymer matrix which are

typically stretchable and transparent. [23-24] Hydrogels, as a type of important ionic conductor, are ideal candidates for soft electrodes of TENGs due to their wide variability, high conductivity, stretchability, transparency, and self-healing ability.[25-26] Wang et al. developed the first skin-like TENG using polyacrylamide (PAAm) hydrogel containing lithium chloride as the conductive electrode. [27] Polyvinyl alcohol (PVA) is another popular hydrogel material due to its high transparency, ease of fabrication, as well as self-healing ability. [28-29] The PVA hydrogel is normally fabricated by crosslinking PVA molecules in water, and the conductivity of PVA hydrogel is enhanced by introducing salt ions into the hydrogel. [29] Lee et al. prepared a self-healing PVA hydrogel, which was crosslinked by borax, and the TENG fabricated using the PVA hydrogel was transparent and stretchable. The Na^+ and $B(OH)_4^-$ ions from borax assisted charge transfer during the operation of the TENG. [30] Although the use of transparent hydrogel as electrodes can result in transparent stretchable TENGs, the effect of hydrogel property on the performance of the TENG is rarely studied.

In the basic TENG working mechanism, repetitive contact and separation of tribopositive and tribonegetive materials triggered the move of electrons back and forth from one electrode to the other electrode through the external circuit.[31-33] Generally, the triboelectric materials play the most important role in determining the output performance of the TENG when metallic electrodes were used in the TENG, since the thin electrode layer which has high conductivity would barely affect the mechanical property of the TENG. [34-35] However, the viscoelastic property of hydrogel is an important property apart from its conductivity, and it may have a significant effect on the TENG performance since TENG is constantly subjected to mechanical stress during operation. Therefore, it is worthy to investigate the influence of the composition and property of the hydrogel electrode on the output performance of the TENG, in order to provide guidelines for the designing of hydrogel-based TENG.

In this study, a hybrid dual-network hydrogel composed of PVA and alginate was prepared and used as the electrode layer in the TENG. The effects of hydrogel properties on the output performance of the hydrogel-based TENG were investigated comprehensively. The optimized hydrogel-based TENG showed a high output voltage of 203.4 V and current of 17.6 μA, and the maximum power density of 0.98 W/m^2 was obtained when the TENG was connected to a 4.7 MΩ resistor. In addition to the outstanding output, the TENG was highly transparent and stretchable. The TENG also showed high continuous running stability and the TENG still maintained a high output voltage of 173 V, when stored in air for 4 weeks.

2. Experimental Methods

2.1 Materials

Polyvinyl alcohol (PVA, Mw 89000−98000, 99%+ hydrolyzed) , calcium chloride, and sodium alginate (SA) were purchased from Sigma-Aldrich (Milwaukee, USA). Sodium tetraborate ($Na_2B_4O_7$, 99.5%) was bought from Fisher Scientific, abbreviated as borax later. All solutions were prepared using deionized water (Milli-Q). Silicone elastomer kit (Sylgard TM 184) was bought from Dow Corning Company. All reagents were used as received.

2.2 Preparation of PVA-SA dual-network hydrogel

The PVA and SA were added into deionized water at predetermined concentration and dissolved at 90 °C for 1 h to make different PVA/SA solutions. The concentration of PVA was 8% wt., and the weight ratio of SA to PVA was 1%, 2%, 3% and 4%, respectively. At the same time, borax solution with concentration of 8% wt was prepared by dissolving borax in water at 50 °C. After the prepared solutions were cooled down to room temperature, borax solution was slowly mixed with the PVA/SA solution using a spatula to prepare the PVA/SA hydrogel. The optimized weight ratio of PVA to borax was 6:1. Then, the prepared hydrogels were immersed into a fresh prepared $CaCl_2$ solution (1 $mol \cdot L^{-1}$) at room temperature for 4 h to

induce ionic crosslinking of the SA. For comparison, pure PVA hydrogel was also prepared following the same protocol.

2.3 Fabrication of hydrogel-based triboelectric nanogenerators (H-TENGs)

The base and crosslinker in the silicone elastomer kit was mixed at a ratio of 10:1, and cast into a polystyrene (PS) dish to form a 1 mm thick layer, then crosslinked for 1 h at 50 °C in an oven to obtain a sticky PDMS film. A PTFE plate (20 mm width × 50 mm length×1 mm thickness) was then placed and semi-embedded in the sticky PDMS film, followed by addition of more PDMS precursor solution into the PS dish to form a sandwiched PDMS bag with total thickness of 2 mm. Then the PS dish was placed into the 50 °C oven for 3 h to fully crosslink the PDMS. A PDMS bag with inner dimension of 20 mm× 50 mm×1 mm was obtained when the PTFE plate was removed. To prepare H-TENGs, different hydrogels were filled into the PDMS bag. An aluminum strand was used as current lead, and a PDMS cap was used to enclose the hydrogel inside the PDMS bag, then the cap was sealed using epoxy glue.

2.4 Characterization of materials and TENGs

The FTIR spectra of the hydrogels prepared were carried out on a Tensor 27 spectrometer (Bruker) with a 4 cm^{-1} resolution. UV-vis spectrum characterization was carried out on a UV−vis spectrophotometer (Cary 500 UV-vis-NIR spectrophotometer), and samples were measured in the range of 800 to 200 nm with blank reference to investigate the transparency of hydrogels and TENGs. The mechanical property of different hydrogels was carried out on a universal instron mechanical tester (Instron 5967, USA, 250 N load). Hydrogels with dimension of 2 cm × 5 cm were stretched at a cross head speed of 5 mm/min until failure. The self-healing behavior of hydrogel was observed using an optical microscope (Nikon Eclipse Ti-S). The conductivity of hydrogels was measured using a four-point conductivity meter (DEDU ST2258C). The viscoelastic properties of different hydrogels were evaluated by a TA AR 2000ex rheometer with parallel plates (diameter: 25 mm, gap: 500 μm). The oscillatory frequency sweep was performed to determine the linear equilibrium modulus

plateau of the hydrogel with an angular frequency ranging from 0.1 to 100 rad/s at 22 °C. The preset strain was kept at 1%. The oscillatory strain amplitude sweep test was performed to determine the linear viscoelastic region of the hydrogel over a sweep of 0.1% to 500% at a fixed frequency of 1 Hz at 22 °C.

The triboelectric output performance of the developed H-TENG was evaluated by compressing with a dynamic shaker (Shiao, SA-JZ) with controlled force and frequency which were regulated by a signal generator and a signal amplifier. The triboelectric performance experiments are carried out at 20 °C at a humidity of 40%. The output voltage signal was recorded using an oscilloscope (Rigol, ZDS3034 Plus) and the output current signal was recorded using a potentiostat (CHI760E). To obtain representative results, separate testes were measured on three samples in triplicates. The results were presented as mean ± standard deviation, and the most representative curves were presented. The current density and power density of the H-TENG on different external resistors were calculated using $P=I/A$, and $P=I^2R/A$, respectively.

3. Results and Discussion

Hydrogel-based TENGs (H-TENGs) have unique advantages due to their stretchability and flexibility. In order to investigate the effect of hydrogel property, various PVA-SA hybrid hydrogels containing dual crosslinking network were synthesized to develop transparent and stretchable H-TENGs and optimize their performances. As depicted in Figure 1a, the synthesized hydrogel consisted of borax crosslinked PVA network and calcium crosslinked alginate network. Both networks are supermolecular networks with reversible ionic bonds which should render the hydrogel self-healing property as well as high elasticity. In addition, widely presented hydrogen bonding in the hydrogel system is also helpful for improving the self-healing ability. Moreover, the hydrogel system contains Na^+ from sodium alginate, Ca^+

and Cl^- ions from calcium chloride, and $B(OH)_4^-$ ions from borax. These ions should greatly enhance the conductivity of hydrogels, which is favorable for improving TENG performance. [36-37]

Fourier transform Infrared Spectroscopy (FTIR) was used to characterize the chemical composition of the synthesized hydrogels. As shown in Figure 1b, compared to raw PVA, the −OH stretching peak (centered around 3319 cm^{-1}) shifted to a higher wavenumber, and the intensity of the peak was enhanced in the PVA hydrogel, demonstrating the presence of hydrogen bonding between the borax and the PVA molecular chains. [28, 38] When SA was introduced to the hydrogel system, it was found that the stretching vibration of the hydroxyl groups shifted to 3296 cm^{-1}, which suggests the hydrogen bonding interactions between PVA and SA molecular chains. Moreover, compared with pure SA, the peak appeared at 1598 cm^{-1} assigned to the stretching vibration of the $-COO^-$ for SA shifted to 1617 cm^{-1} for PVA-SA, indicating the ionic bonding between Ca^{2+} and $-COO^-$ of SA. [39] The formation of these reversible supermolecular bonds in the hydrogel is desired for improving the stretchability and self-healing performance. As shown in Figure 1c, the prepared PVA-SA hydrogel can be easily stretched to 1000 % strain. Figure 1d shows the self-healing process of the hydrogel. It can be seen the cutting edge almost disappeared when the two pieces were brought into contact for 60 min indicating excellent self-healing ability. The tensile properties of different hydrogels are listed in Table S1 and representative tensile curves are shown in Figure S1. It is obvious that both tensile modulus and tensile strength were improved as the increase of SA concentration, indicating the introduction of alginate network significantly increased the hydrogel crosslinking sites and improved its stiffness. It was found that when the hydrogels are pulled at a higher speed, they maintained good stretchability over 1200%, but the modulus and strength were slightly higher. This was because the molecular chains had less time to relax at a high stretching rate.

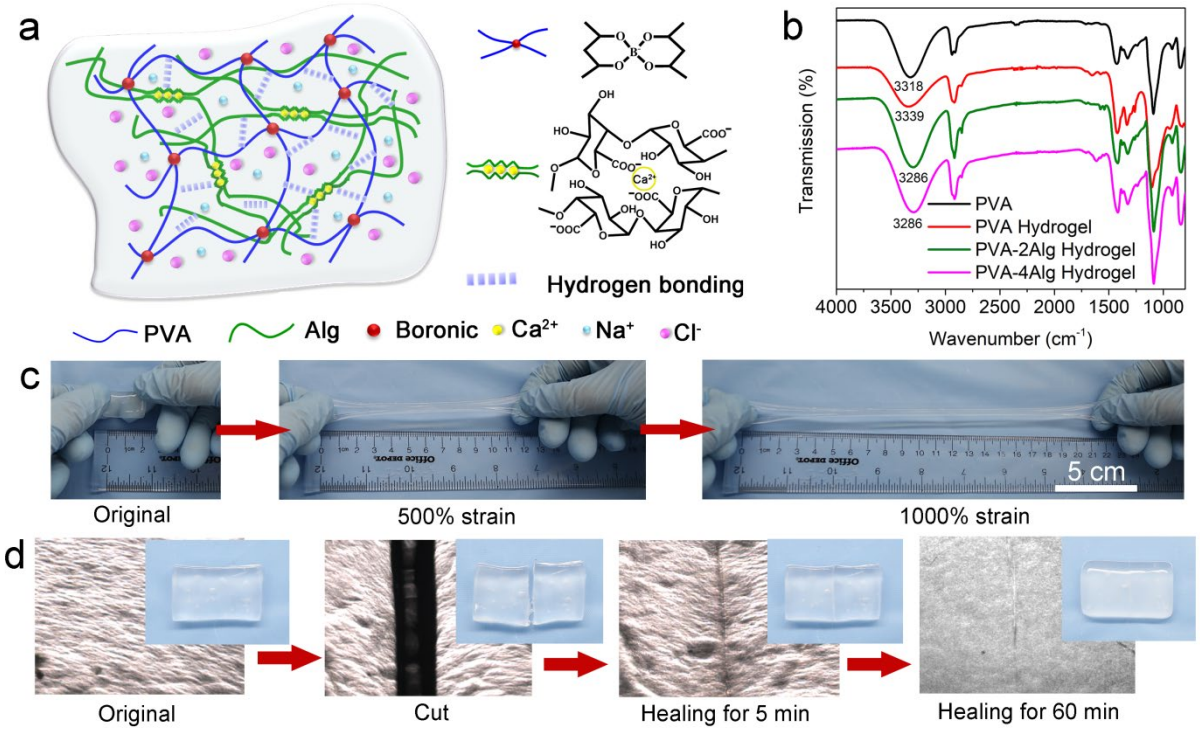

Figure 1. (a) Schematic illustration of the synthesized PVA-SA hydrogel showing the dual crosslink network; (b) FTIR spectra of PVA, PVA hydrogel, and PVA-SA hydrogels; (c) digital photograph showing the high stretch ability of the hydrogel; (d) optical microscope images and relevant photographs showing the self-healing process of the hydrogel.

The output performance deterioration caused by hydrogel dehydration is a critical issue for H-TENG. In order to prevent hydrogel dehydration, as shown in Figure 2, a thin PDMS bag with 1 mm interior thickness was fabricated using a home-made mold in this study. PDMS was chosen because of its high tribonegativity. [40-41] Hydrogel film was filled in the PDMS bag and an aluminum current lead was attached to the hydrogel. A single-electrode H-TENG is obtained after sealing the PDMS bag using a PDMS cap and epoxy glue. The fabricated H-TENG is highly flexible and highly transparent. It can be easily bent or folded to any shape (Figure 2b). As shown in Figure 2c, the as-prepared hydrogel has transparency close to 100%, and the H-TENG still maintains high transparency over 90%. Moreover, the

H-TENG still possesses high stretchability. As demonstrated in Figure 2d, the H-TENG can be easily stretched to 250% strain.

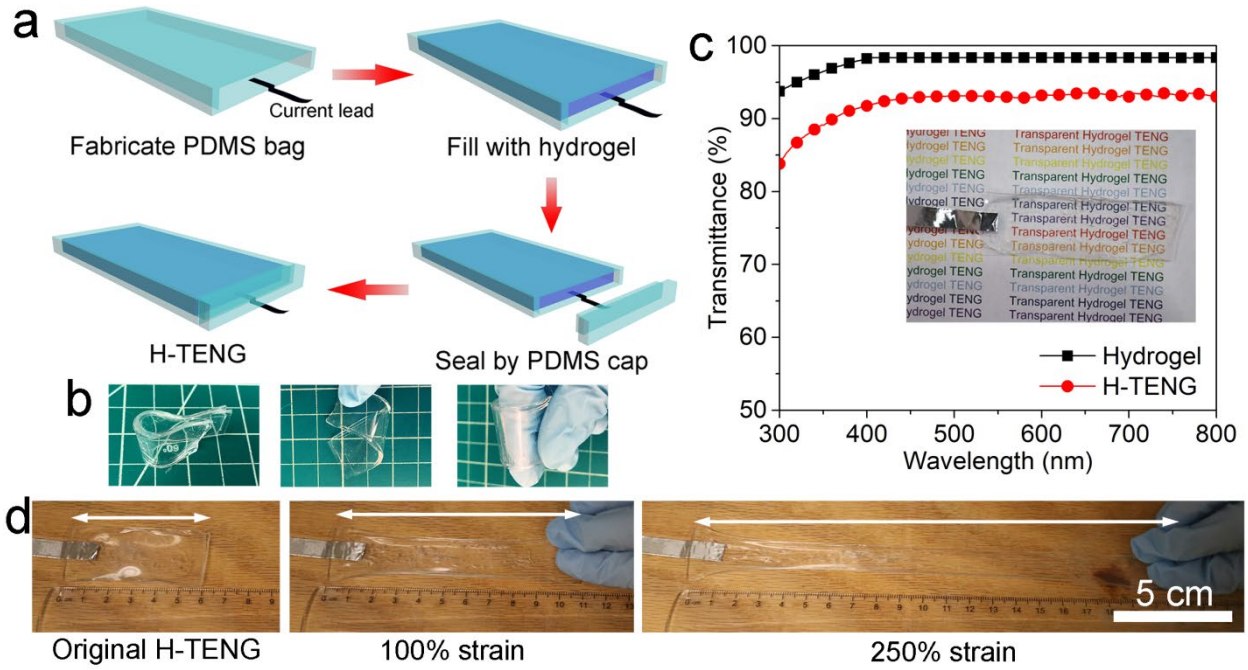

Figure 2. (a) Illustration of the hydrogel-based TENG fabrication procedure; (b) digital photos showing the high transparency and flexibility of the TENG; (c) UV-vis spectra of the hydrogel and hydrogel-based TENG; (d) The stretchbility of the fabricated H-TENG.

Due to the high tribonegativity of PDMS, H-TENG can generate energy when it is in contact with any material that is more tribopositive relative to PDMS. We chose aluminum as the counterpart to investigate the effect of different hydrogels on the output performance of the H-TENG. As depicted in Figure 3a, when aluminum is in contact with the H-TENG, PDMS is negatively charged and the aluminum is positively charged at the same time due to the contact electrification effect. When the material separates, an electrostatic potential difference is created, which leads to the redistribution of ions in the hydrogel. Due to the attraction of negative charges on PDMS, sodium cations move toward the negative charges while chloride anions move toward the negative direction. Therefore, electrons are pushed out through the grounded external circuit (single-electrode working mode) and caused an instant

current flow. When the positively charged aluminum is moving towards the H-TENG again, the electrostatic potential difference is offset, and electrons are attracted back through the grounded external circuit which results in another instant current flow in the opposite direction. Comparing the different hydrogels, as shown in Figure 3b, it was found that the output voltage increased as the increase of the SA concentration in the hydrogel, and the highest output voltage of (98.6 V) was achieved on the H-TENG composed of hydrogel containing 2% SA. When the alginate concentration is further increased, the output voltage was reduced to 29.8 V which is even lower than the PVA hydrogel (Figure S2). It was found that the trend maintained the same for the short circuit current results as shown in Figure 3c and Figure S3. The maximum current of 7.3 μA was obtained on the H-TENG composed of hydrogel containing 2% SA.

The H-TENG can also work in double-electrodes mode by simply connecting the current lead to the aluminum layer. As depicted in Figure 3d, once the hydrogel is connected to the aluminum layer, electrons flowed back and forth from the current lead to the aluminum layer as continuous contacting and separating of aluminum layer and the H-TENG. From Figure 3e and f, it was found that the output voltage and current were both higher in the double-electrode working mode. Moreover, the same trends maintained for H-TENGs made of different hydrogels in double-electrode working mode. The maximum voltage of 203.4 V and the maximum current of 17.6 μA are achieved on the H-TENG composed of hydrogel containing 2% SA. The output voltage and current are almost doubled when the H-TENGs are working in double-electrode mode compared with the performance in single-electrode mode (Figure S4 and S5). This was because the electrostatic potential difference in single-electrode mode is the difference between PDMS and ground, while the electrostatic potential difference in double-electrode mode is the difference between PDMS and aluminum, which is about twice of the potential difference in single-electrode mode. Therefore, it is favorable to complete double-electrode circuit in practical application as far as circumstances permit.

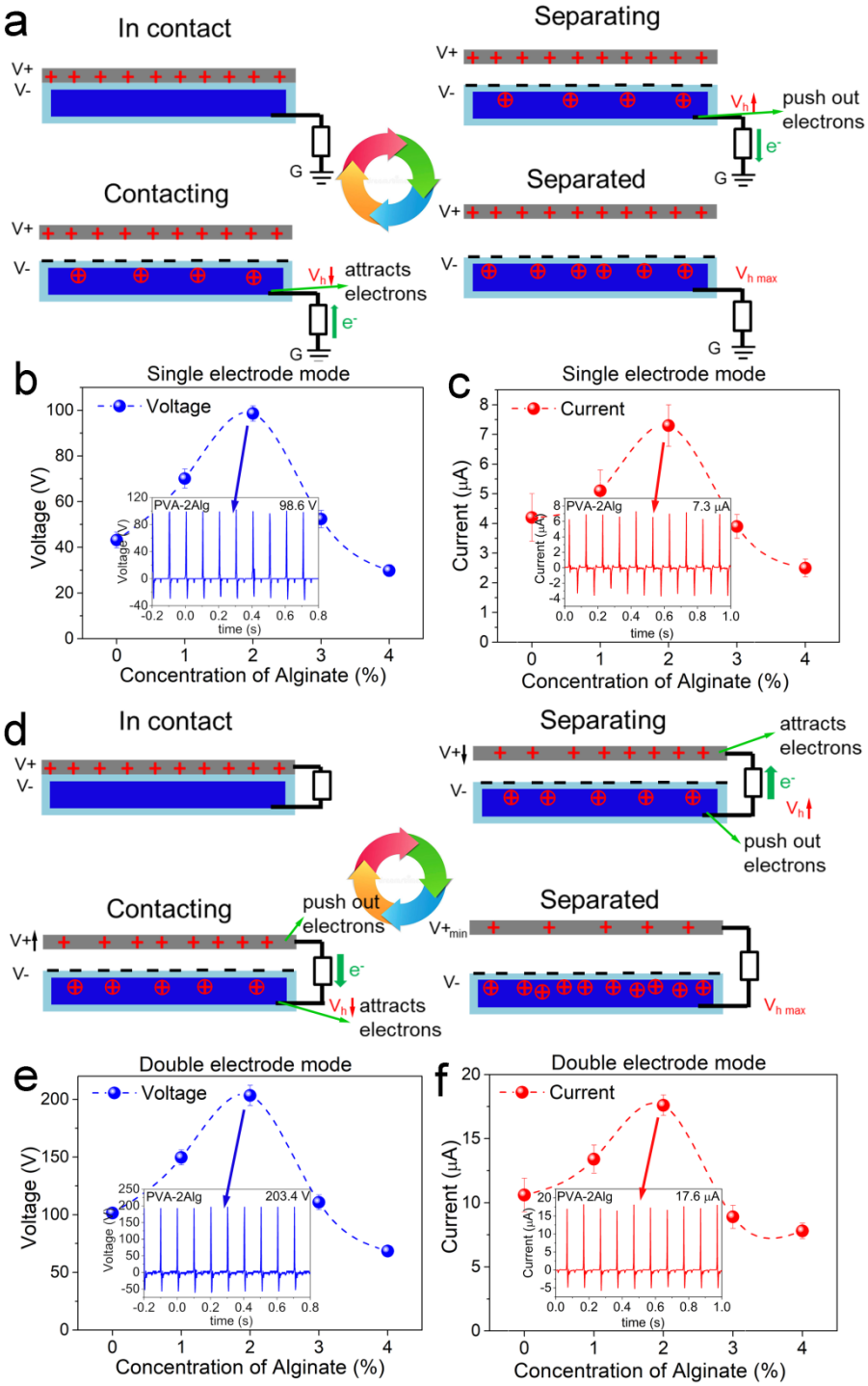

Figure 3. (a) Working principle of the TENG in single-electrode mode; (b) the maximum instant output voltage of different H-TENGs in single-electrode mode; (c) the maximum instant output current of different H-TENGs in single-electrode mode; (d) working principle of the TENG in double-electrodes mode; (e) the maximum instant output voltage of different H-TENGs in double-electrode mode; (f) the maximum instant output current of different H-TENGs in double-electrode mode

The experiment results showed that the hydrogel property in H-TENG had a significant effect on the output performance. It was found that the conductivity of hydrogel increased as the increase of SA concentration due to the increased concentration of sodium and chloride ions (Figure 4a). While interestingly, the triboelectric output performance did not continuously increase as the increase of hydrogel conductivity. It is believed that the viscoelastic property of the hydrogel may be an important factor affecting the triboelectric performance.

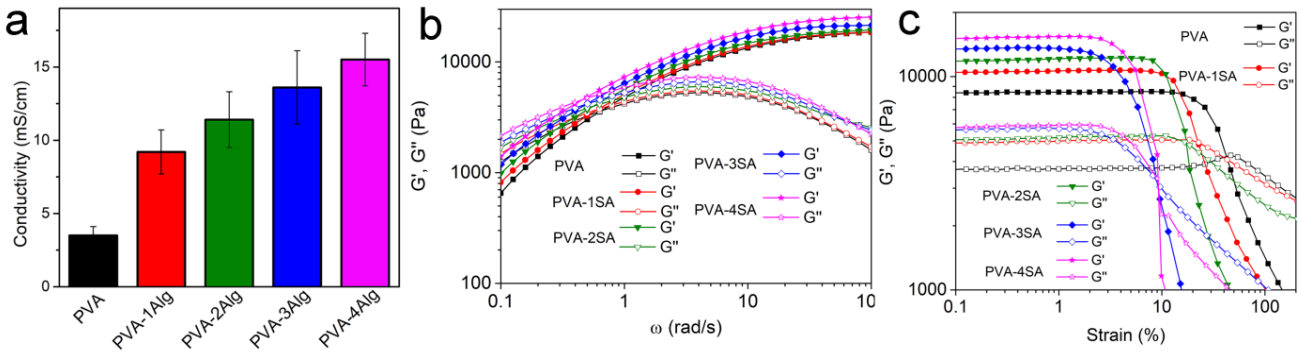

Figure 4. (a) Conductivity results of different hydrogels; (b) storage and loss modulus of different hydrogels in oscillation frequency sweep; (c) storage and loss modulus of different hydrogels in strain sweep.

As shown in Figure 4b, the storage modulus (G') of the hydrogel increased as the increase of SA content in the hydrogel, while the loss modulus (G") was increased first at low frequency and decreased at high frequency. The intersects of G' and G" curves represent the transformation of hydrogels from liquid-like behavior to solid-like behavior. The relaxation time t_r (t_r=1/ω_c, ω_c is the crossover frequency), which implies the ability for hydrogel network to relax, reflects the mobility of hydrogel molecular chains (overall crosslinking stiffness). As shown in Table 1, the relaxation time was increased as the SA concentration increase in the hydrogel. Greater t_r was ascribe to longer lifetime of the cross-links under physical forces,

denser entanglements or a higher crosslink density. [42] Furthermore, the strain sweep measurements (Figure 4c) showed that all hydrogels had a linear viscoelastic region (*LVR*) at low strain. *LVR*, which is represented by the crossover strain of storage and loss modulus, indicates the elastic response range of hydrogels. From Table 1, it was found that PVA-SA hydrogel displays a much narrower *LVR* compared to pure PVA hydrogel, demonstrating a shortened elastic response range, which was ascribed to the high rigidity of the alginate network. [43] For PVA-SA hydrogels, steep change of both t_r and *LVR* happened when the SA concentration was increased from 2% to 3%. This indicated a significant transformation of dual crosslinking network from elastic to be more rigid. Thus, the hydrogel with SA concentration over 3% should be more difficult to adapt deformation upon dynamic forces. It was found the triboelectric output of PVA-4SA hydrogel-based H-TENG was even lower than neat PVA hydrogel-based H-TENG, although it possesses much higher conductivity. In another word, PVA-2SA hydrogel would have superior elastic response when subjected to periodic tapping forces, which resulted in superior triboelectric performance of PVA-2SA hydrogel-based H-TENG. Moreover, it was noticed that the PVA hydrogel showed an increase of G'' in the end of linear region, which indicates the increase of plasticity of molecular chains in the end of linear region. This implies that the borax crosslinking of hydroxyl groups of PVA was not stable at high strain. However, the G'' increase was absent when alginate Ca^{2+} crosslinking network was introduced to the hydrogel, which means the dual-crosslinking network is more stable under high strain. Since charges are generated on the PDMS layer and the hydrogel was placed beneath the PDMS, the mechanical property of hydrogel would affect the charges generated on PDMS. A hydrogel with high elasticity would lead to soft contact during the TENG operation, which is beneficial for improving the contact electrification effect by increasing the chance of charge transfer, and enhancing the TENG performance. [44]. In this study, we have verified that hydrogels with high elasticity supposed to

be more favorable for ionic electrodes in H-TENGs compared to rigid hydrogels, which would be useful for directing the design of TENGs.

Table 1. Relaxation time (t_r) and linear viscoelastic region (LVR) of different hydrogels

	PVA	**PVA-1SA**	**PVA-2SA**	**PVA-3SA**	**PVA-4SA**
t_r **(s)**	1.57	1.65	1.77	2.09	2.22
LVR **(%)**	43.21	22.37	17.97	9.2	8.83

Next, we focused on investigating the performance of H-TENG based on PVA-2SA hydrogel. For a single-electrode H-TENG, the material in contact with H-TENG determines the output performance of the device. The H-TENG was tested against a variety of materials (Figure 5a) to account for its performance in various circumferences, it was found that the output voltage when pressed using dry hand was the highest, and the output voltage trend generally followed the triboelectric series. The results suggested that the H-TENG can harvest mechanical energy from the motion of different materials. Figure 5b demonstrated the H-TENG has a sensitive response to the compressing force as well. And the output voltage increased significantly as the increase of pressing force. Moreover, the output voltage of the H-TENG was very stable, when operated at different frequencies (from 2 Hz to 20 Hz) as shown in Figure 5c, which indicates that the instant energy output is highly synergistic to the pressing events, and the response of the H-TENG is highly effective. To demonstrate the stability of the H-TENG, it was continuously run for 30 min and it was found from Figure 5d that the output voltage maintained about the same during operation, suggesting excellent performance stability. In addition, the dehydration of hydrogel is the major issue of H-TENGs. The weight loss and the performance change of the H-TENG were investigated for up to 28 days. As shown in Figure 5e, the weight loss of the hydrogel was very slow and the weight loss was within 4% even 28 days after the H-TENG was prepared due to the tight sealing using the PDMS bag. It should be note that the hydrogel contains about 90% water according

to the synthesis procedure, and the hydrogel would totally dry out in 2-3 days when exposed in air. Although no significant weight loss was observed, the output voltage was gradually decreased from 201 V to 173 V from day 1 to day 28 as shown in Figure 5f, and it is believed that this decrease was caused by the hardening of the hydrogel. Nevertheless, the H-TENG developed significantly hindered dehydration and improved the performance stability. Moreover, the output performance of the dehydrated H-TENG can be easily regained by simply soaking it in water for 2 days and drying its surface with tissue paper (Figure S6).

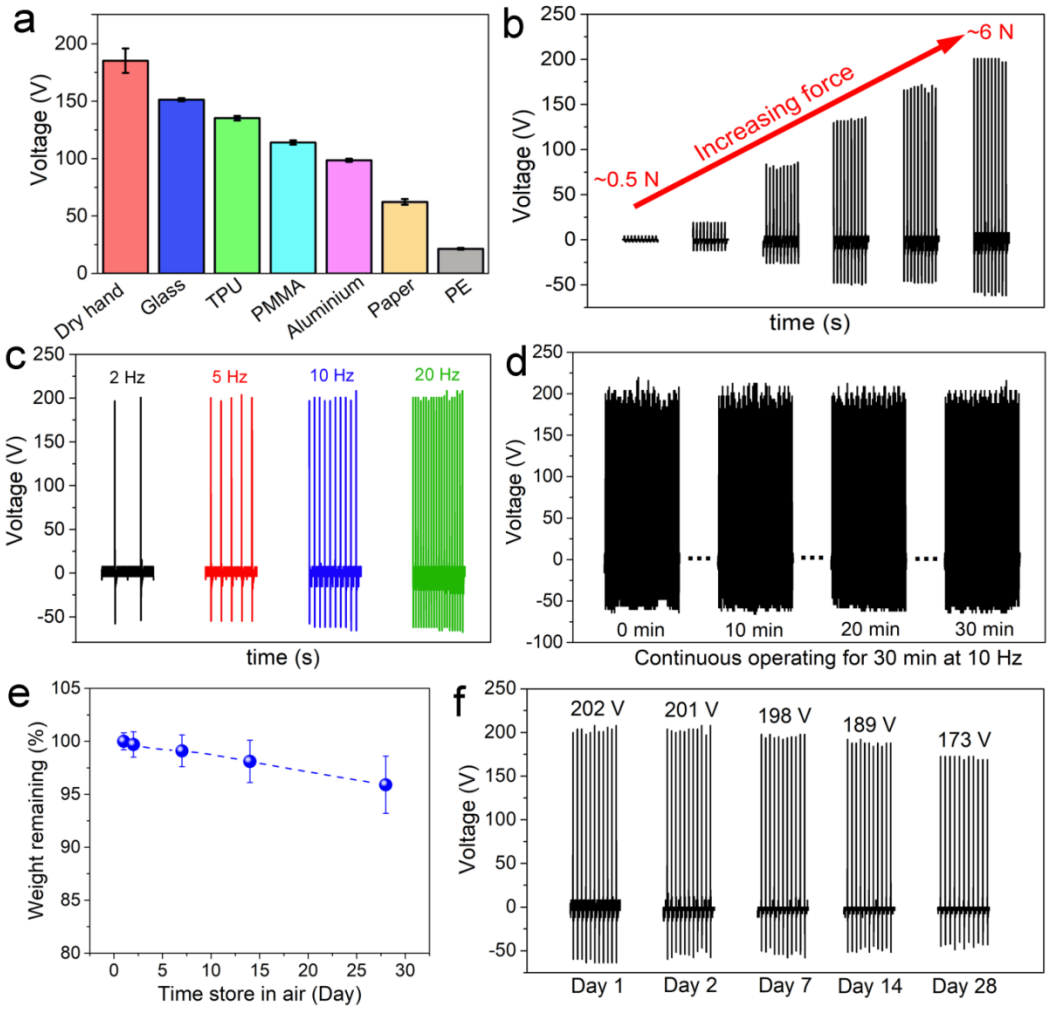

Figure 5. (a) The output voltage of the H-TENG against different materials; (b) output voltage of the H-TENG when compressed with different force at 10 Hz; (c) output voltage of the H-TENG when compressed at different frequency; (d) output voltage signal of the H-TENG during 30 min continuous running; (e) weight remaining of the H-TENG when stored

in air for 4 weeks to reflect water loss; (f) output voltage of the H-TENG when stored in air for 4 weeks.

The H-TENG fabricated has high stretchability, and it can be easily stretched to 200% of its original length. As shown in Figure 6a, the output voltage decreased as the increase of stretch ratio, but a highly stable output signal was maintained. This was mainly because the contact area was reduced during the test as shown in Figure S7. Moreover, the reduction of the hydrogel conductivity due to the decrease of cross section area may be another reason for the output voltage decrease. Since the output voltage decreases as the increase of stretching ratio, the developed H-TENG has the potential to be used as a strain sensor. To evaluate the output performance of the H-TENG in the external circuit, it was connected to resistors with different resistances as external load. As shown in Figure 6b, the current density decreased as the increase of external load resistance. The power density was increased as the increase of external resistance at low resistance since the current change was insignificant. When the resistance was further increased, the power density started decreasing because of the rapid reduction of current. A maximum power density of 0.98 W/m^2 was achieved on a 4.7 MΩ resistor. The high power density of the H-TENG is suitable for powering various small devices and light LEDs. As shown in Figure 6c and Movie 1, the fabricated H-TENG can easily light 240 green and blue LEDs when pressed with aluminum. Similarly, the same amount of LEDs can be lit using bare hand pressing when the H-TENG is operating in a single-electrode mode (Movie 2). As shown in Figure S8, a high voltage of about 200 V can be achieved using dry hand pressing.

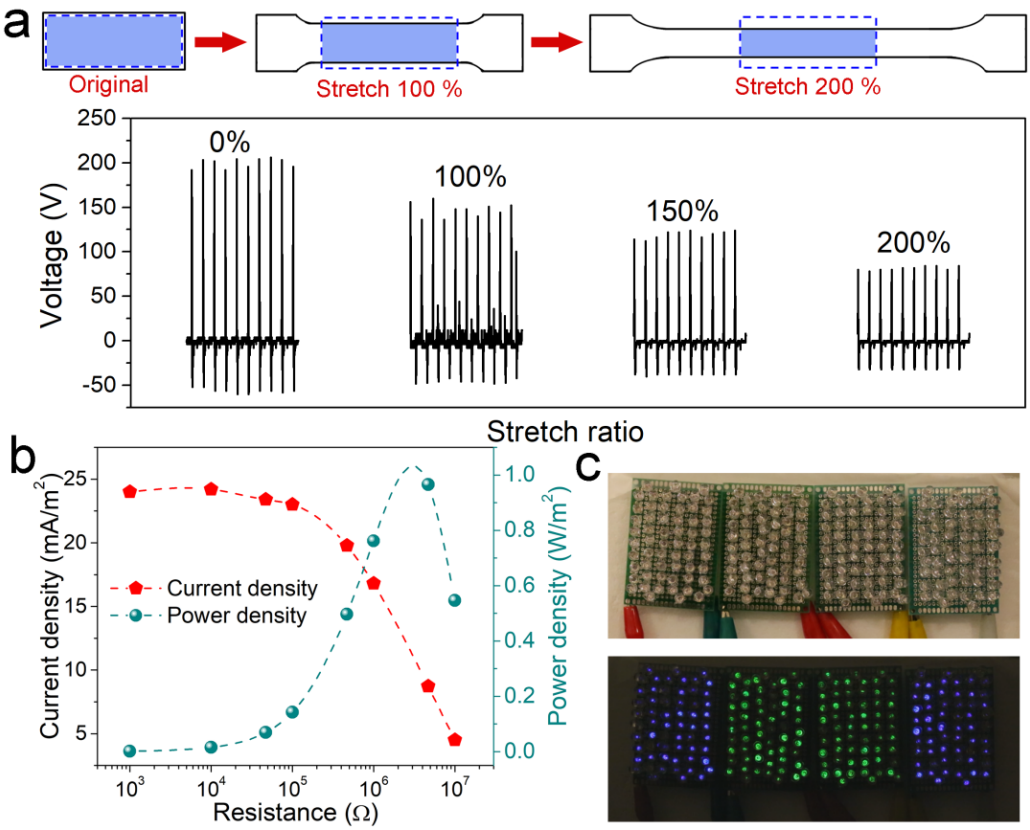

Figure 6. (a) Output voltage of H-TENG when been stretched to 100%, 150%, and 200% strain; (b) current density and power density of the H-TENG when connected to external resistors with different resistance; (c) The H-TENG was able to light 240 green and blue LEDs when compressed using aluminum or dry hand.

Since the H-TENG generates periodic alternating voltage, it is difficult to directly use the energy generated by H-TENG as a power source for devices. Therefore, the H-TENG was connected to a capacitor through a bridge rectifier as shown in Figure 7a. It was found that the H-TENG was able to charge a 22 μF capacitor to 7.2 V in 180 s, and charge a 330 μF capacitor to 1.6 V in 616 s, when pressed using aluminum at 10 Hz. When a 10 μF capacitor is charged to 6.3 V by the H-TENG, the energy could light two white LEDs for ~3s (Figure S9). The harvested energy can also be used to power small devices like a digital timer as shown in Figure 7b and Movie 3. However, the energy generation rate was not fast enough to compensate for the energy consumption by the timer. When a 22 μF capacitor was charged to

2.2 V, the energy is enough to power the timer for ~ 4 s, and a ~ 23 s resting time is necessary for the capacitor to be charged to 2.2 V again. It is expected that the timer can be continuously powered if five H-TENG was connected in parallel. [34] Alternatively, we can use a larger capacitor and longer charging time to increase the device operating time. As shown in Figure 7c and Movie 4, the H-TENG could charge a 1000 μF capacitor to 1.6 V in 25 min, and the energy is sufficient to continuously power a pedometer.

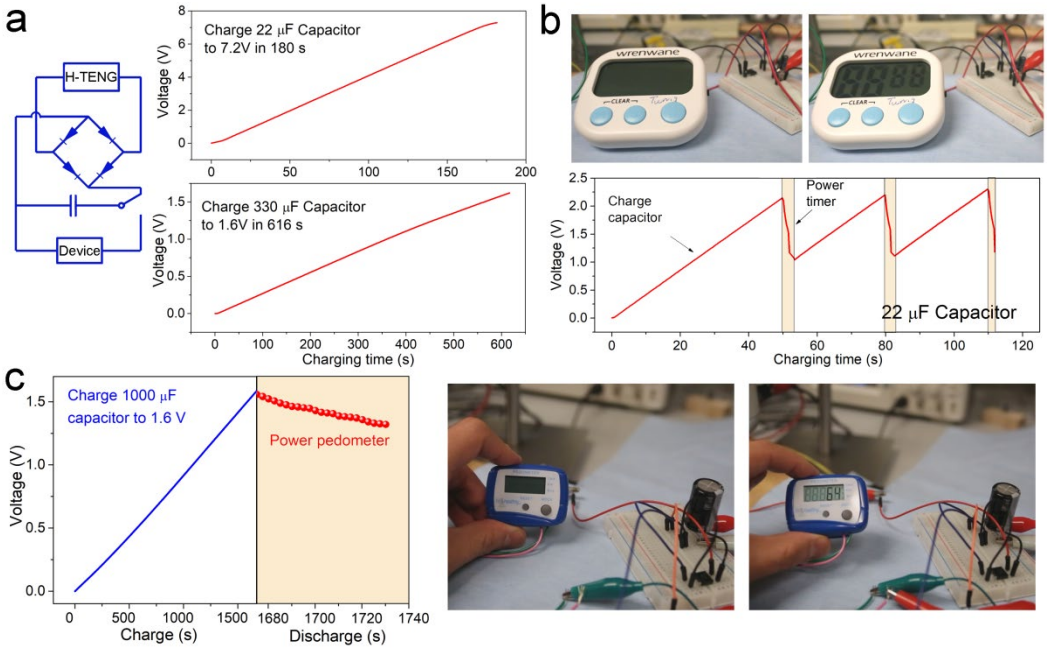

Figure 7. (a) the H-TENG can be used to charge capacitors through a bridge rectifier; (b) the H-TENG was used to charge a 22μF capacitor to 2.2 V and intermittently power a digital timer; (c) the H-TENG was used to charge a 1000 μF capacitor to 1.6 V and continueously power a pedometer.

4. Conclusion

PVA-SA dual crosslinking network hydrogel-based H-TENGs with high transparency (over 90%) and stretchability (over 250%) were developed in this study. The effects of hydrogel composition and property on the triboelectric output performance were investigated specifically. Enhancing conductivity is favorable for improving H-TENG output, while the

viscoelasticity is also an important property affecting the H-TENG performance. For the first time, it was found that elastic hydrogel-based H-TENG showed superior output performance than rigid hydrogel-based H-TENG due to its elastic response when subjected to the external force. With optimized hydrogel composition, maximum output voltage and current of 203.4 V and 17.6 μA were obtained when compressed using aluminum foil. The specially designed H-TENG could effectively prevent dehydration and maintain a stable output in continuous operation. The output voltage reduction of the H-TENG was within 15% after 4 weeks exposer in the atmosphere. The H-TENG achieved a relatively high power density of 0.98 W/m^2 when connected to a 4.7 MΩ resistor. The energy generated can be used to light up to 240 green and blue LEDs. The H-TENG also demonstrated the ability to quickly charge capacitors with capacitance up to 1000 μF through a bridge rectifier, and the energy can be used to power small electronics, such as a digital timer and pedometer.

Acknowledgements

The authors would like to acknowledge the financial support of the National Natural Science Foundation of China (51603075; 21604026), and the support of the following two grants from Research Grants Council of Hong Kong. 1) “Proactive monitoring of work-related MSD risk factors and fall risks of construction workers using wearable insoles” (PolyU 152099/18E); and 2) In search of a suitable tool for proactive physical fatigue assessment: an invasive to non-invasive approach. (PolyU 15204719/18E).

Supporting Information

Supplementary data associated with this article can be found, in the online version.

Mechanical property, additional output voltage and current data, output after rehydration, performance using hand tapping, and additional demonstration. (PDF)

H-TENG power 240 green and blue LEDs by taping using aluminum. (Movie 1)

H-TENG power 240 green and blue LEDs by hand tapping. (Movie 2)

Power a digital timer using a 22 μF capacitor charged by the H-TENG. (Movie 3)

Power a pedometer using a 1000 μF capacitor charged by the H-TENG. (Movie 4)

References

(1) Tang, Y. F.; Zheng, Q. F.; Chen, B.; Ma, Z. Q.; Gong, S. Q. A new class of flexible nanogenerators consisting of porous aerogel films driven by mechanoradicals. *Nano Energy* **2017,** *38*, 401-411.

(2) Dudem, B.; Kim, D. H.; Bharat, L. K.; Yu, J. S. Highly-flexible piezoelectric nanogenerators with silver nanowires and barium titanate embedded composite films for mechanical energy harvesting. *Appl Energ* **2018,** *230*, 865-874.

(3) Guo, H. Y.; Yeh, M. H.; Lai, Y. C.; Zi, Y. L.; Wu, C. S.; Wen, Z.; Hu, C. G.; Wang, Z. L. All-in-One Shape-Adaptive Self-Charging Power Package for Wearable Electronics. *Acs Nano* **2016,** *10* (11), 10580-10588.

(4) Fan, F. R.; Tang, W.; Wang, Z. L. Flexible Nanogenerators for Energy Harvesting and Self-Powered Electronics. *Adv. Mater.* **2016,** *28* (22), 4283-4305.

(5) Wang, Z. L.; Jiang, T.; Xu, L. Toward the Blue Energy Dream by Triboelectric Nanogenerator Networks. *Nano Energy* **2017,** *39*, 9-23.

(6) Yang, J.; Chen, J.; Yang, Y.; Zhang, H. L.; Yang, W. Q.; Bai, P.; Su, Y. J.; Wang, Z. L. Broadband Vibrational Energy Harvesting Based on a Triboelectric Nanogenerator. *Adv. Energy Mater.* **2014,** *4* (6), 1301322.

(7) Zhao, L. Y.; Yang, Y. W. An Impact-based Broadband Aeroelastic Energy Harvester for Concurrent Wind and Base Vibration Energy Harvesting. *Appl Energ* **2018,** *212*, 233-243.

(8) Li, Z. J.; Saadatnia, Z.; Yang, Z. B.; Naguib, H. A Hybrid Piezoelectric-triboelectric Generator for Low-frequency and Broad-bandwidth Energy Harvesting. *Energ Convers Manage* **2018,** *174*, 188-197.

(9) Chen, B. D.; Tang, W.; He, C.; Deng, C. R.; Yang, L. J.; Zhu, L. P.; Chen, J.; Shao, J. J.; Liu, L.; Wang, Z. L. Water Wave Energy Harvesting and Self-powered Liquid-surface Fluctuation Sensing Based on Bionic-jellyfish Triboelectric Nanogenerator. *Mater Today* **2018,** *21* (1), 88-97.

(10) Wang, W. C.; Xu, J. C.; Zheng, H. W.; Chen, F. Q.; Jenkins, K.; Wu, Y. H.; Wang, H. Y.; Zhang, W. F.; Yang, R. S. A Spring-assisted Hybrid Triboelectric-electromagnetic

Nanogenerator for Harvesting Low-frequency Vibration Energy and Creating a Self-powered Security System. *Nanoscale* **2018,** *10* (30), 14747-14754.

(11) Shao, Y.; Feng, C. P.; Deng, B. W.; Yin, B.; Yang, M. B. Facile Method to Enhance Output Performance of Bacterial Cellulose Nanofiber Based Triboelectric Nanogenerator by Controlling Micro-nano Structure and Dielectric Constant. *Nano Energy* **2019,** *62*, 620-627.

(12) Wen, Z.; Yang, Y. Q.; Sun, N.; Li, G. F.; Liu, Y. N.; Chen, C.; Shi, J. H.; Xie, L. J.; Jiang, H. X.; Bao, D. Q.; Zhuo, Q. Q.; Sun, X. H. A Wrinkled PEDOT:PSS Film Based Stretchable and Transparent Triboelectric Nanogenerator for Wearable Energy Harvesters and Active Motion Sensors. *Adv. Funct. Mater.* **2018,** *28* (37), 1803684.

(13) Markvicka, E. J.; Bartlett, M. D.; Huang, X. N.; Majidi, C. An Autonomously Electrically Self-healing Liquid Metal-elastomer Composite for Robust Soft-matter Robotics and Electronics. *Nat. Mater.* **2018,** *17* (7), 618-624.

(14) Shao, Y.; Luo, C.; Deng, B. W.; Yin, B.; Yang, M. B. Flexible Porous Silicone Rubber-nanofiber Nanocomposites Generated by Supercritical Carbon Dioxide Foaming for Harvesting Mechanical Energy. *Nano Energy* **2020,** *67*, 104290.

(15) Parida, K.; Thangavel, G.; Cai, G. F.; Zhou, X. R.; Park, S.; Xiong, J. Q.; Lee, P. S. Extremely Stretchable and Self-healing Conductor Based on Thermoplastic Elastomer for All-three-dimensional Printed Triboelectric Nanogenerator. *Nat Commun* **2019,** *10*, 2158

(16) Fang, H. J.; Wang, X. D.; Li, Q.; Peng, D. F.; Yan, Q. F.; Pan, C. F. A Stretchable Nanogenerator with Electric/Light Dual-Mode Energy Conversion. *Adv. Energy Mater.* **2016,** *6* (18), 1600829.

(17) Liang, X. W.; Zhao, T.; Jiang, W.; Yu, X. C.; Hu, Y. G.; Zhu, P. L.; Zheng, H. R.; Sun, R.; Wong, C. P. Highly Transparent Triboelectric Nanogenerator Utilizing In-situ Chemically Welded Silver Nanowire Network as Electrode for Mechanical Energy Harvesting and Body Motion Monitoring. *Nano Energy* **2019,** *59*, 508-516.

(18) Shi, J. H.; Chen, X. P.; Li, G. F.; Sun, N.; Jiang, H. X.; Bao, D. Q.; Xie, L. J.; Peng, M. F.; Liu, Y. N.; Wen, Z.; Sun, X. H. A Liquid PEDOT:PSS Electrode-based Stretchable Triboelectric Nanogenerator for a Portable Self-charging Power Source. *Nanoscale* **2019,** *11* (15), 7513-7519.

(19) Lee, J.; Lee, P.; Lee, H.; Lee, D.; Lee, S. S.; Ko, S. H. Very Long Ag Nanowire Synthesis and Its Application in a Highly Transparent, Conductive and Flexible Metal Electrode Touch Panel. *Nanoscale* **2012,** *4* (20), 6408-6414.

(20) Zhao, G. R.; Zhang, Y. W.; Shi, N.; Liu, Z. R.; Zhang, X. D.; Wu, M. Q.; Pan, C. F.; Liu, H. L.; Li, L. L.; Wang, Z. L. Transparent and Stretchable Triboelectric Nanogenerator for Self-powered Tactile Sensing. *Nano Energy* **2019,** *59*, 302-310.

(21) Chen, H. M.; Xu, Y.; Zhang, J. S.; Wu, W. T.; Song, G. F. Enhanced Stretchable Graphene-based Triboelectric Nanogenerator via Control of Surface Nanostructure. *Nano Energy* **2019,** *58*, 304-311.

(22) Liu, T.; Liu, M. M.; Dou, S.; Sun, J. M.; Cong, Z. F.; Jiang, C. Y.; Du, C. H.; Pu, X.; Hu, W. G.; Wang, Z. L. Triboelectric-Nanogenerator-Based Soft Energy-Harvesting Skin Enabled by Toughly Bonded Elastomer/Hydrogel Hybrids. *Acs Nano* **2018,** *12* (3), 2818-2826.

(23) Parida, K.; Xiong, J. Q.; Zhou, X. R.; Lee, P. S. Progress on Triboelectric Nanogenerator with Stretchability, Self-healability and Bio-compatibility. *Nano Energy* **2019,** *59*, 237-257.

(24) Sun, L. J.; Chen, S.; Guo, Y. F.; Song, J. C.; Zhang, L. Z.; Xiao, L. J.; Guan, Q. B.; You, Z. W. Ionogel-based, Highly Stretchable, Transparent, Durable Triboelectric Nanogenerators for Energy Harvesting and Motion Sensing over a Wide Temperature range. *Nano Energy* **2019,** *63*, 103847.

(25) Guan, Q. B.; Lin, G. H.; Gong, Y. Z.; Wang, J. F.; Tan, W. Y.; Bao, D. Q.; Liu, Y. N.; You, Z. W.; Sun, X. H.; Wen, Z.; Pan, Y. Highly Efficient Self-healable and Dual Responsive Hydrogel-based Deformable Triboelectric Nanogenerators for Wearable Electronics. *J. Mater. Chem. A* **2019,** *7* (23), 13948-13955.

(26) Lee, Y.; Cha, S. H.; Kim, Y. W.; Choi, D.; Sun, J. Y. Transparent and Attachable Ionic Communicators Based on Self-cleanable Triboelectric Nanogenerators. *Nat Commun* **2018,** *9*, 1804

(27) Pu, X.; Liu, M.; Chen, X.; Sun, J.; Du, C. H.; Zhang, Y.; Zhai, J.; Hu, W.; Wang, Z. L. Ultrastretchable, Transparent Triboelectric Nanogenerator as Electronic Skin for Biomechanical Energy Harvesting and Tactile Sensing. *Science Advances* **2017,** *3* (5), e1700015.

(28) Jing, X.; Li, H.; Mi, H. Y.; Liu, Y. J.; Feng, P. Y.; Tan, Y. M.; Turng, L. S. Highly Transparent, Stretchable, and Rapid Self-healing Polyvinyl Alcohol/Cellulose Nanofibril Hydrogel Sensors for Sensitive Pressure Sensing and Human Motion Detection. *Sensor Actuat B-Chem* **2019,** *295*, 159-167.

(29) Xu, W.; Huang, L. B.; Wong, M. C.; Chen, L.; Bai, G. X.; Hao, J. H. Environmentally Friendly Hydrogel-Based Triboelectric Nanogenerators for Versatile Energy Harvesting and Self-Powered Sensors. *Adv. Energy Mater.* **2017,** *7* (1), 1601529.

(30) Parida, K.; Kumar, V.; Wang, J. X.; Bhavanasi, V.; Bendi, R.; Lee, P. S. Highly Transparent, Stretchable, and Self-Healing Ionic-Skin Triboelectric Nanogenerators for Energy Harvesting and Touch Applications. *Adv. Mater.* **2017,** *29* (37), 1702181.

(31) Wu, C. S.; Wang, A. C.; Ding, W. B.; Guo, H. Y.; Wang, Z. L. Triboelectric Nanogenerator: A Foundation of the Energy for the New Era. *Adv. Energy Mater.* **2019,** *9* (1), 1802906.

(32) Mi, H. Y.; Jing, X.; Zheng, Q.; Fang, L.; Huang, H. X.; Turng, L. S.; Gong, S. High-Performance Flexible Triboelectric Nanogenerator Based on Porous Aerogels and Electrospun Nanofibers for Energy Harvesting and Sensitive Self-Powered Sensing. *Nano Energy* **2018,** *48*, 327-336.

(33) Zhai, C.; Chou, X. J.; He, J.; Song, L. L.; Zhang, Z. X.; Wen, T.; Tian, Z. M.; Chen, X.; Zhang, W. D.; Niu, Z. C.; Xue, C. Y. An Electrostatic Discharge Based Needle-to-needle Booster for Dramatic Performance Enhancement of Triboelectric Nanogenerators. *Appl Energ* **2018,** *231*, 1346-1353.

(34) Mi, H. Y.; Jing, X.; Meador, M. A. B.; Guo, H. Q.; Turng, L. S.; Gong, S. Q. Triboelectric Nanogenerators Made of Porous Polyamide Nanofiber Mats and Polyimide Aerogel Film: Output Optimization and Performance in Circuits. *ACS Appl. Mater. Interfaces* **2018,** *10* (36), 30596-30606.

(35) Mi, H. Y.; Jing, X.; Cai, Z. Y.; Liu, Y. J.; Turng, L. S.; Gong, S. Q. Highly Porous Composite Aerogel based Triboelectric Nanogenerators for High Performance Energy Generation and Versatile Self-powered Sensing. *Nanoscale* **2018,** *10* (48), 23131-23140.

(36) Wang, X. D.; Zhang, Y. F.; Zhang, X. J.; Huo, Z. H.; Li, X. Y.; Que, M. L.; Peng, Z. C.; Wang, H.; Pan, C. F. A Highly Stretchable Transparent Self-Powered Triboelectric Tactile Sensor with Metallized Nanofibers for Wearable Electronics. *Adv. Mater.* **2018,** *30* (12), 1706738.

(37) Yang, C. H.; Suo, Z. G. Hydrogel Ionotronics. *Nat Rev Mater* **2018,** *3* (6), 125-142.

(38) Cai, G. F.; Wang, J. X.; Qian, K.; Chen, J. W.; Li, S. H.; Lee, P. S. Extremely Stretchable Strain Sensors Based on Conductive Self-Healing Dynamic Cross-Links Hydrogels for Human-Motion Detection. *Adv Sci* **2017,** *4* (2), 1600190.

(39) Hua, S. B.; Ma, H. Z.; Li, X.; Yang, H. X.; Wang, A. pH-sensitive Sodium Alginate/Poly(vinyl alcohol) Hydrogel Beads Prepared by Combined Ca2+ Crosslinking

and Freeze-thawing Cycles for Controlled Release of Diclofenac Sodium. *Int J Biol Macromol* **2010,** *46* (5), 517-523.

(40) Rasel, M. S. U.; Park, J. Y. A sandpaper Assisted Micro-structured Polydimethylsiloxane Fabrication for Human Skin Based Triboelectric Energy Harvesting Application. *Appl Energ* **2017,** *206*, 150-158.

(41) Trinh, V. L.; Chung, C. K. Harvesting Mechanical Energy, Storage, and Lighting Using a Novel PDMS Based Triboelectric Generator with Inclined Wall Arrays and Micro-topping Structure. *Appl Energ* **2018,** *213*, 353-365.

(42) Han, J. Q.; Lei, T. Z.; Wu, Q. L. High-water-content Mouldable Polyvinyl Alcohol-borax Hydrogels Reinforced by Well-dispersed Cellulose Nanoparticles: Dynamic Rheological Properties and Hydrogel Formation Mechanism. *Carbohyd Polym* **2014,** *102*, 306-316.

(43) Li, X. F.; Shu, M. M.; Li, H.; Gao, X.; Long, S. J.; Hu, T.; Wu, C. G. Strong, Tough and Mechanically Self-recoverable Poly(vinyl alcohol)/Alginate Dual-physical Double-network Hydrogels with Large Cross-link Density Contrast. *Rsc Adv* **2018,** *8* (30), 16674-16689.

(44) Xu, C.; Zi, Y. L.; Wang, A. C.; Zou, H. Y.; Dai, Y. J.; He, X.; Wang, P. H.; Wang, Y. C.; Feng, P. Z.; Li, D. W.; Wang, Z. L. On the Electron-Transfer Mechanism in the Contact-Electrification Effect. *Adv. Mater.* **2018,** *30* (15), 1706790.

Table of Content

Highly stretchable and transparent hydrogel-based triboelectric nanogenerators (H-TENGs) based on dual crosslinking network ionic hydrogels were developed. The hydrogel viscoelastic property realized significant effects on the H-TENG output performance. The hydrogel with high elasticity and conductivity showed optimum output voltage and current of 203.4 V and 17.6 μA, and achieved a peak power density of 0.98 W/m^2. The H-TENG has high stability in continuous operation and can simultaneously light 240 LEDs and power small electronics. The study provides insights into the designing of high performance stretchable and transparent H-TENGs